Ingledew, W. J., Reid, G. A., Poole, R. K., Blum, H., & Ohnishi, T. (1980) *FEBS Lett. 111*, 223.
Jaworowski, A., Campbell, H. D., Poulis, M. I., & Young, I. G. (1981a) *Biochemistry 20*, 2041.
Jaworowski, A., Mayo, G., Shae, D. C., Campbell, H. D., & Young, I. G. (1981b) *Biochemistry 20*, 3621.
Matsushita, K., & Kaback, H. R. (1986) *Biochemistry 25*, 2321.
Matsushita, K., Patel, L., Gennis, R. B., & Kaback, H. R. (1983) *Proc. Natl. Acad. Sci. U.S.A. 80*, 4889.
Matsushita, K., Patel, L., & Kaback, H. R. (1984) *Biochemistry 23*, 4703.
Murakami, H., Kita, K., Oya, H., & Anraku, Y. (1985) *FEMS Microbiol. Lett. 30*, 307.
Owen, P., & Kaback, H. R. (1978) *Proc. Natl. Acad. Sci. U.S.A. 75*, 3148.
Owen, P., & Kaback, H. R. (1979a) *Biochemistry 18*, 1413.
Owen, P., & Kaback, H. R. (1979b) *Biochemistry 18*, 1422.
Owen, P., Kaczorowski, G. J., & Kaback, H. R. (1980a) *Biochemistry 19*, 596.
Owen, P., Kaback, H. R., & Graeme-Cook, K. A. (1980b) *FEMS Microbiol. Lett. 7*, 345.
Poole, R. K., & Haddock, B. A. (1975) *Biochem. J. 152*, 537.
Ramos, S., Schuldiner, S., & Kaback, H. R. (1976) *Proc. Natl. Acad. Sci. U.S.A. 73*, 1892.
Reenstra, W. W., Patel, L., Rottenberg, H., & Kaback, H. R. (1980) *Biochemistry 19*, 1.
Schaffner, W., & Weissman, C. (1973) *Anal. Biochem. 56*, 502.
Waggoner, A. (1979) *Annu. Rev. Biophys. Bioeng. 8*, 47.
Young, I. G., Jaworowski, A., & Poulis, M. I. (1978) *Gene 4*, 25.
Young, I. G., Rogers, B. L., Campbell, H. D., Jaworowski, A., & Shaw, D. C. (1981) *Eur. J. Biochem. 116*, 165.

Raman Spectroscopy of Interferon-Induced 2′,5′-Linked Oligoadenylates†

Joseph C. White, Robert W. Williams, and Margaret I. Johnston*
Department of Biochemistry, The Uniformed Services University of the Health Sciences, Bethesda, Maryland 20814-4799
Received March 23, 1987; Revised Manuscript Received June 2, 1987

ABSTRACT: Raman spectra of model compounds and of 2′,5′-oligoadenylates in D_2O were utilized to assign the Raman bands of 2′,5′-oligoadenylates. The Raman spectra of A2′pA2′pA, pA2′pA2′pA, and pppA2′pA2′pA contained features that were similar to those of adenosine, adenosine 5′-monophosphate (AMP), and adenosine 5′-triphosphate, respectively. When AMP and pA2′pA2′pA were titrated from pH 2 to 9, the normalized Raman intensity of their ionized (980 cm^{-1}) and protonated (1080 cm^{-1}) phosphate bands revealed similar pK_a's for the 5′-monophosphates. The Raman spectrum of pA2′pA2′pA was altered slightly by elevations in temperature, but not in a manner supporting the postulate that 2–5A possesses intermolecular base stacking. Major differences in the Raman spectrum of 2′,5′- and 3′,5′-oligoadenylates were observed in the 600–1200-cm^{-1} portion of the spectrum that arises predominately from ribose and phosphate vibrational modes. Phosphodiester backbone modes in A3′pA3′pA and pA3′pA3′pA produced a broad band at 802 cm^{-1} with a shoulder at 820 cm^{-1}, whereas all 2′,5′-oligoadenylates contained a major phosphodiester band at 823 cm^{-1} with a shoulder at 802 cm^{-1}. The backbone mode of pppA2′pA2′pA contained the sharpest band at 823 cm^{-1}, suggesting that the phosphodiester backbone may be more restrained in the biologically active, 5′-triphosphorylated molecule. The Raman band assignments for 2′,5′-oligoadenylates provide a foundation for using Raman spectroscopy to explore the mechanism of binding of 2′,5′-oligoadenylates to proteins.

Interferons are recognized as important biological mediators that have numerous effects on the immune system, including inhibition of viral replication. Interferons induce at least two double-stranded RNA-dependent proteins, 2′,5′-oligoadenylate synthetase and protein P_1 kinase [reviewed by Johnston and Torrence (1984)]. 2′,5′-Oligoadenylate synthetase polymerizes ATP[1] into pppA(2′pA)$_n$, where $n \geq 2$ (2–5A). 2′,5′-Oligoadenylates activate a latent endoribonuclease (RNase L) that degrades RNA and contributes to the translational inhibition caused by double-stranded RNA (dsRNA) (Kerr & Brown, 1978; Kerr et al., 1974; Lebleu et al., 1976; Sen et al., 1976).

The unique nature of these 2′,5′-oligoadenylates has prompted investigation into the structural requirements for

† This work was supported in part by The Uniformed Services University of the Health Sciences (Grant T07146 to J.C.W. and Grant GM 7159 to M.I.J.) and the National Science Foundation (Grant PCM-8443154 to R.W.W.). The opinions or assertions contained herein are the private ones of the authors and are not to be construed as official or reflecting the views of the U.S. Department of Defense or The Uniformed Services University of the Health Sciences.
* Author to whom correspondence should be addressed.

[1] Abbreviations: 2–5A (trimer triphosphate), 5′-*O*-triphosphoryladenylyl(2′,5′)adenylyl(2′,5′)adenosine [pppA2′p(A2′p)$_n$A, where n is usually 1–3]; pA2′pA2′pA (trimer monophosphate), 5′-*O*-monophosphoryladenylyl(2′,5′)adenylyl(2′,5′)adenosine; pA2′pA3′pA, 5′-*O*-monophosphoryladenylyl(2′,5′)adenylyl(3′,5′)adenosine; pA3′pA2′pA, 5′-*O*-monophosphoryladenylyl(3′,5′)adenylyl(2′,5′)adenosine; A2′pA2′pA (trimer core), adenylyl(2′,5′)adenylyl(2′,5′)adenosine; A3′pA3′pA, adenylyl(3′,5′)adenylyl(3′,5′)adenosine; pA2′pA^{8Br}2′pA^{8Br}, 5′-*O*-monophosphoryladenylyl(2′,5′)-8-bromoadenylyl-8-bromoadenosine; dsRNA, double-stranded RNA; RNase L, 2–5A-dependent endoribonuclease; HEPES, 4-(2-hydroxyethyl)-1-piperazineethanesulfonic acid; AMP, adenosine 5′-monophosphate; ADP, adenosine 5′-diphosphate; ATP, adenosine 5′-triphosphate; HPLC, high-performance liquid chromatography; CD, circular dichroism; NMR, nuclear magnetic resonance.

their binding to and activation of RNase L. The number of 5′-phosphates was shown to be important in determining the biological activity of 2–5A. Trimer 5′-triphosphate, pppA2′pA2′pA, and trimer 5′-diphosphate, ppA2′pA2′pA, bind and activate RNase L. Trimer 5′-monophosphate, pA2′pA2′pA, binds the endonuclease but does not activate the enzyme, and trimer core, A2′pA2′pA, neither binds nor activates RNase L efficiently (Kerr & Brown, 1978; Torrence et al., 1981). However, trimer core at high concentrations has been implicated in the inhibition of DNA and RNA synthesis, although the mechanism of core action remains unclear (Kimchi et al., 1981a,b). More detail on the portions of 2–5A critical to binding and activation of RNase L have been obtained through the study of structural analogues of 2–5A. Efficient binding to RNase L requires the N6 amino group of the 5′-terminal adenine (Torrence et al., 1984; Imai & Torrence, 1985; Imai et al., 1985) and two 2′,5′-phosphodiester bonds (Lesiak et al., 1983). Activation of RNase L requires the N6 amino group of the 2′-terminal adenine (Torrence et al., 1984; Imai & Torrence, 1985; Imai et al., 1985) and the 3′-OH of the ribose ring (Sawai et al., 1983; Haugh et al., 1983). An analogue brominated at the C8 position of adenine, pA2′pA^{8Br}2′pA^{8Br}, displayed unexpected biological activity. This 5′-monophosphate shows significant binding and activation of RNase L (Torrence et al., 1985; Torrence & Lesiak, 1986). This unexpected result demonstrates that biological activity does not always require a 5′-terminal di- or triphosphate and implies that the biological activity of different 2′,5′-oligoadenylates may be dictated by a structural feature other than the number of 5′-terminal phosphates.

Early Raman spectroscopic studies of mononucleotides (Lord & Thomas, 1967) have led to the emergence of Raman spectroscopy as a useful method for studying nucleic acid structure. The technique requires small but concentrated samples that may be in the form of crystal, film, fiber, or aqueous solution. Raman spectroscopy has proven useful in distinguishing differences in nucleic acid structure. For example, characteristic Raman "marker" bands have been described for the A, B, C, and Z forms of DNA (Erfurth et al., 1972, 1975; Benevides & Thomas, 1983; Benevides et al., 1984). Raman spectroscopy may also be employed to study nucleic acid binding reactions. Ligand–DNA (Manfait et al., 1984) and protein–cofactor (Yue et al., 1986) binding complexes have been evaluated by using Raman difference spectra. Difference spectra provide information concerning which part of the ligand or cofactor interacts with the DNA or protein.

We describe here a qualitative assignment of the Raman bands of the interferon-induced 2′,5′-oligoadenylates based on Raman spectra of model compounds and of 2′,5′-oligoadenylates under various conditions. Defining the vibrational modes that are responsible for the bands in the Raman spectrum of 2–5A is an obligatory first step in studies designed to explore the molecular binding interactions between 2–5A and proteins. We also observe that the phosphodiester backbone of the biologically active form of 2–5A, pppA2′pA2′pA, differs from those of the inactive forms of 2–5A and of 3′,5′-oligoadenylates.

Materials and Methods

Commercial 2′,5′-linked trimer core, A2′pA2′pA, trimer 5′-monophosphate, pA2′pA2′pA, and trimer 5′-triphosphate, pppA2′pA2′pA (ammonium salts), were purchased from Pharmacia Chemical Co. (Piscataway, NJ). Synthetic 2′,5′-linked trimer core and trimer 5′-monophosphate (sodium salt) were generously supplied by Dr. Paul F. Torrence (NIH). Adenosine (Sigma grade), AMP (Sigma grade), and ATP (Sigma grade) were purchased from Sigma Chemical Co. (St. Louis, MO). All samples were dissolved in distilled water or in buffer containing 150 mM NaCl and 10 mM HEPES, pH 7.4. Sample concentration was estimated spectroscopically and ranged from 10 to 100 mM. Raman experiments were carried out at 15 °C except where noted otherwise. The temperature of the brass sample holder was maintained by a thermostatically controlled circulating water bath.

The Raman instrument consisted of a Coherent Innova 90 argon ion laser operating at 514.5 nm with typically 250 mW of light power at the sample, a thermostated brass sample holder, a 300-mm focal length f 0.6 aspheric lens for light collection optics, a Spex 1403 double monochrometer with 1800 grooves/mm holographic gratings, an RCA 31034 PMT, and a Spex Datamate coupled to a Cromemco Z80 based microcomputer. Spectral band-pass was set to 6 cm^{-1}. Data was collected at 1-cm^{-1} intervals at a scan rate of 1 cm^{-1}/s. About 15 scans were collected on each spectrum with a 2 s/cm^{-1} integration time. Samples of approximately 5 μL were held in melting point capillary tubes. Spectra containing significant noise were 5 point smoothed according to the algorithm of Savitsky and Golay (1967). Water and solvent background peaks, including those from HEPES where appropriate, were subtracted from spectra as described by Williams (1983).

To ensure that samples were pure and were not degraded by the laser beam, by changes in pH, or by high temperatures employed in certain experiments, samples were analyzed by C-18 reverse-phase HPLC. Less than 1 μL of sample was removed from each melting point capillary tube before and after scanning and diluted approximately 20-fold for analysis. The HPLC system consisted of a Waters Model 730 data module, a Waters Model 720 system controller, a Waters Model 710B WISP, two Waters Model 510 solvent delivery systems, and a Kratos Model 769 variable wavelength detector. Buffer A was 50 mM ammonium acetate, pH 5.2, and buffer B was 25% acetonitrile. The flow rate was 1 mL/min. The column was a Waters μBondapak C-18 3.0 mm × 30 cm stainless steel column. The gradient was programed as follows: 0–5 min, 100% A; 5–25 min, shallow exponential gradient (curve 07) to 25% B; 25–35 min, steeper exponential gradient (curve 08) to 100% B. Absorbance was monitored at 259 nm. Average retention times in minutes were as follows: pppA2′pA2′pA, 27.2; ppA2′pA2′pA, 24.0; pA2′pA2′pA, 24.2; A2′pA2′pA, 35.6; A2′pA, 34.4; AMP, 9.2; adenosine, 29.9.

Sample pH was measured by insertion of a specially constructed combination pH electrode, measuring 0.9 mm (diameter) by 6.0 cm (length) (Microelectrodes, Inc., Londonderry, NH), into the melting point capillary tube. Accurate pH measurements were made on volumes as low as 2 μL and were done in duplicate. There was no significant difference in the pH of a 5-μL sample, determined as described above, and the pH of 1 mL of the same sample measured in a test tube. Sample pH was changed by delivering less than 1 μL of ice-cold 0.1 N KOH to the inside of the capillary tube with the tip of the pH electrode. The electrode and sample were kept on ice to minimize possible base-mediated degradation. This procedure changed the pH by about 0.5 unit per addition step without degrading the sample. The ionized 980-cm^{-1} and protonated 1095-cm^{-1} phosphate peak heights were measured after each spectrum was normalized to the 729-cm^{-1} band of adenine by using data handling programs described by Williams (1983).

Samples scanned in D_2O were lyophilized and reconstituted on ice with D_2O from Sigma. The sample was immediately

Table I: Raman Active Modes for Model and 2′,5′-Linked Compounds

obsd Raman frequency shift[a] (cm^{-1})						calcd frequency shift[b] (cm^{-1})	potential energy distribution[c]
adenosine	A2′pA2′pA	AMP	pA2′pA2′pA	ATP	pppA2′p-A2′pA		
1650		1650		1650			C=N (19), C—C (25), C—N (23), N—C= (19)
1582	1580	1580	1578	1585	1580	1581	C5C4 (48) - C4N3 (31)
1512	1510	1510	1510	1515	1510	1531	C5C4 (25) - C2N3 (23)
1486	1480	1482	1480	1487	1480	1468	δC2H (29) - N9C8 (19) + δC8H
1458	1460	1460	1458	1462	1460	1464	ribosyl CH_2 bending[d]
1428	1422	1422	1422	1422	1425	1689	C4N (44) - δC8H (15)
1378	1378	1378	1378	1380	1380	1351	C—N (50), C=C (16)
1340	1340	1340	1340	1340	1340	1329	N7C5 (39) + C8N7 (12)
1308	1310	1308	1305	1305	1310	1309	N9C8 (30) + N3C2 (14) + δC8H (14) - δC2H
1254	1254	1254	1254	1254	1254	1424	N1C6 (31) + C6N6′(26)
1214	1220	1220	1218	1220	1222	1218	adenine ring bending
1178	1180	1180	1180	1180	1178	1171	N1—C2—N3 (25), N1—C2 (23), C2=N3 (14), N6—C6=N1 (14)
				1113	1115	1125	PO_3^{2-} 5′-triphosphate[e]
	1085		1075		1080		O–P–O symmetric diester stretch[d]
1005	1010	1000	1010	1015	1010		adenine torsion
		980	980				PO_3^{2-} 5′-monophosphate[e]
			918	918	918		not assigned
	880	882	895	892	890		not assigned
865							not assigned
		854		855	850		asymmetric O–P–O,[d] backbone[e]
	825	822	825	830	825		not assigned
		802	802	805	802		symmetric O–P–O[d]
	780		795		780		C4—N9—C1′(16), C1′O5′ (11)
729	729	729	729	729	729	681	δN7C8N9 (19) - N9 ribose (14) + δC5N7C8 (12) + δC4N9C8 (11)
630	638	640	638	640	640		backbone-A bending

[a] Frequency shifts experimentally observed in this paper. [b] Frequency shifts assigned by normal mode analysis by Fodor et al. (1985) and/or Baret et al. (1979). [c] Potential energy distributions based on normal mode analysis by Fodor et al. (1985) and/or Baret et al. (1979), except where noted otherwise. [d] Assignment from Thomas et al. (1983). [e] Assignment from Rimai et al. (1969).

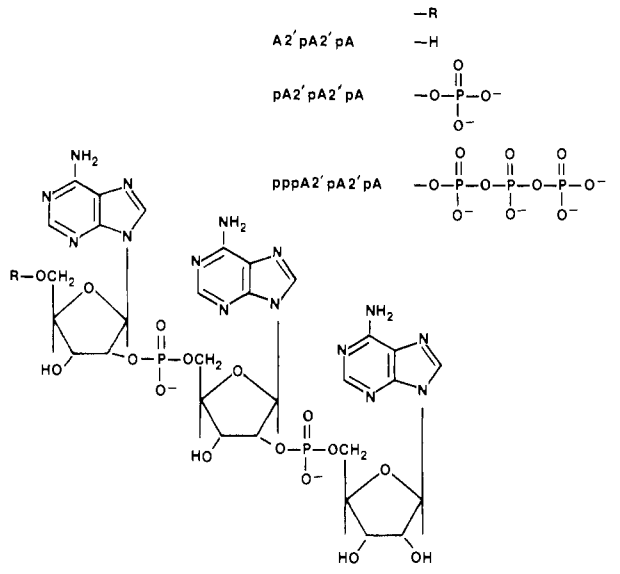

FIGURE 1: Schematic of 2′,5′-oligoadenylates. R = H for A2′pA2′pA, R = PO_3^{2-} for pA2′pA2′pA, and R = $P_3O_{10}^{4-}$ for pppA2′pA2′pA2.

transferred to the thermostated 15 °C brass sample holder for Raman analysis.

RESULTS

General Characteristics of Raman Spectra of 2–5A. The structures of 2′,5′-oligoadenylates are depicted in Figure 1. A clear relationship between the Raman spectrum of each model compound, adenosine, AMP, and ATP, and the Raman spectrum of 2′,5′-oligoadenylates A2′pA2′pA, pA2′pA2′pA, and pppA2′pA2′pA can be seen in Figure 2. These spectra contain bands that originate from vibrational modes of the 5′-monophosphate at 980 cm^{-1} (Figure 2C,D) (Rimai et al., 1969), the 5′-triphosphate at 1125 cm^{-1} (Figure 2E,F) (Rimai et al., 1969), the phosphodiester backbone at 800–880 cm^{-1}

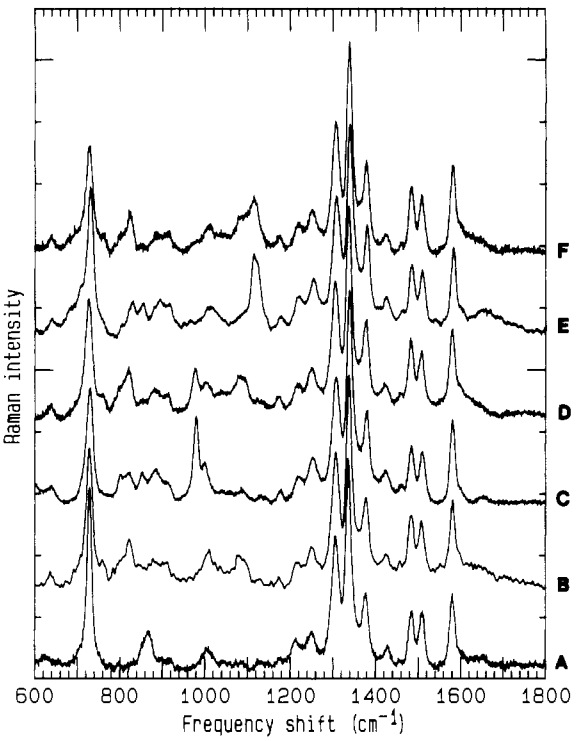

FIGURE 2: Raman spectra of 2′,5′-oligoadenylates and model compounds: (A) adenosine in saline HEPES, pH 7.4; (B) A2′pA2′pA in water, pH 7.3; (C) AMP in water, pH 7.3; (D) pA2′pA2′pA in water, pH 7.3; (E) ATP in water, pH 7.3; (F) pppA2′pA2pA in water, pH 7.3. Samples were prepared and scanned as described under Materials and Methods.

(Brown & Peticolas, 1975; Thomas & Peticolas, 1983), and the adenine bases at 729 and 1200–1600 cm^{-1} (Lord & Thomas, 1967; Rimai et al., 1969; Baret et al., 1979; Fodor et al., 1985). Thus, the major differences in the Raman spectra

of A2′pA2′pA, pA2′pA2′pA, and pppA2′pA2′pA result from differences in the 5′-terminus and the ribose phosphate backbone.

The major Raman active modes for model compounds and 2′,5′-oligoadenylates at pH 7.3 are summarized in Table I. Ring vibrations were identified by comparison with the frequencies reported for nucleotide monomers (Lord & Thomas, 1967; Fodor et al., 1985; Rimai et al., 1969) and polynucleotides (Baret et al., 1979). Backbone vibrations were identified by comparison with normal coordinate calculations (Brown & Peticolas, 1975; Shimanouchi et al., 1964; Lu et al., 1975). These results show excellent correlation with previously published data on A3′pA3′pA and poly(riboadenylic acid) (Small & Peticolas, 1971; Prescott et al., 1974).

Adenine-Related Modes. Modes above 1240 cm^{-1} arise from vibrations of adenine bases (Table I). Minor differences between the observed Raman frequency of base bands in the spectra of model compounds and 2–5A may arise from the coupling through the N9–C2′ bond. Bands at 1308, 1340, 1378, 1422–1428, 1482–1484, 1510–1515, and 1580–1585 cm^{-1} have been identified previously as adenine ring modes (Lord & Thomas, 1967; Rimai et al., 1969; Baret et al., 1979; Fodor et al., 1985). Peaks at 630–640 and 729 cm^{-1} also arise from the adenine ring, although the width of the 729-cm^{-1} peak may be slightly affected by the state of 5′-phosphorylation (Rimai et al., 1969).

Preliminary studies suggested that a 1455-cm^{-1} band in 2′,5′-trimer 5′-monophosphate pA2′pA2′pA (NIH source) originated from the base moieties (Johnston et al., 1985). However, this 1455-cm^{-1} band originates from a triethylammonium ion present from the synthesis or purification of the compound. Subtracting the Raman spectrum of triethylammonium bicarbonate from the Raman spectrum of pA2′pA2′pA (NIH source) resulted in a corrected spectrum that was essentially the same as the Raman spectrum of commercial pA2′pA2′pA (result not shown).

Phosphate Modes. Phosphate mode assignments of 5′-phosphorylated 2′,5′-oligoadenylates were made by comparison with Raman spectra of AMP, ATP, and A2′pA2′pA (Rimai et al., 1969; Yue et al., 1986). Bands for 5′-monophosphates at 980 cm^{-1} and for triphosphates at 1125 cm^{-1} were observed in AMP and ATP and in 2′,5′-oligoadenylates.

The effect of pH on the ionization state of pA2′pA2′pA as reflected by the 980-cm^{-1} (ionized) and 1084-cm^{-1} (protonated) phosphate bands was investigated to determine if the 5′-terminal phosphate of pA2′pA2′pA interacts with other portions of the 2–5A molecule. Such interactions might be expected to alter the pK_a of the 5′-terminal phosphate group. The pH was varied from 2.0 to 9.0. Spectra were normalized to the 729-cm^{-1} adenine base band, which is not affected in intensity or frequency by changes in pH from 5 to 7 (Rimai et al., 1969) or from pH <3 to >5 (Lord & Thomas, 1967; results not shown). The 729-cm^{-1} band in pA2′pA2′pA was also not affected by changes in pH from 2 to 9 (results not shown). The band at 980 cm^{-1} in the control Raman spectrum of AMP showed an apparent pK_a of 6.05 (Figure 3A). The band at 980 cm^{-1} in the Raman spectrum of pA2′pA2′pA showed a similar pK_a of 6.1.

The 1455-cm^{-1} band due to the triethylammonium ion observed in the synthetic pA2′pA2′pA from NIH showed no change in intensity with pH (Figure 3B) relative to the 729-cm^{-1} adenine base band. This further supports the validity of normalizing spectra to the 729-cm^{-1} band.

Deuteriation Effects. The spectra of trimer monophosphate, pA2′pA2pA, in H_2O and in D_2O are compared in Figure 4.

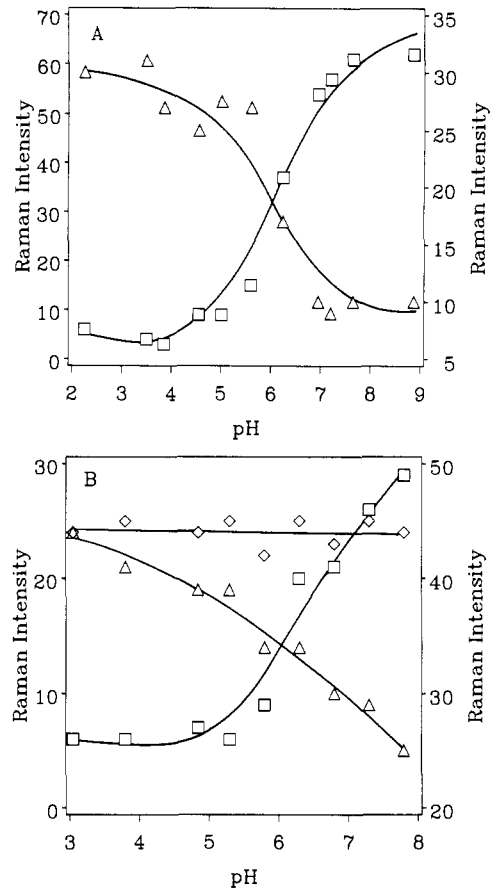

FIGURE 3: Effect of pH on the phosphate modes of AMP and pA2′pA2′pA. (A) Raman intensity of the phosphate modes of AMP, 980 (□) and 1080 (△) cm^{-1}. (B) Raman intensity of pA2′pA2′pA, 980 (□), and 1080 (△), and 1455 (◇) cm^{-1}. Ten units was added to the 1455-cm^{-1} intensities. Spectra were normalized to the 729-cm^{-1} band of adenine as described under Materials and Methods.

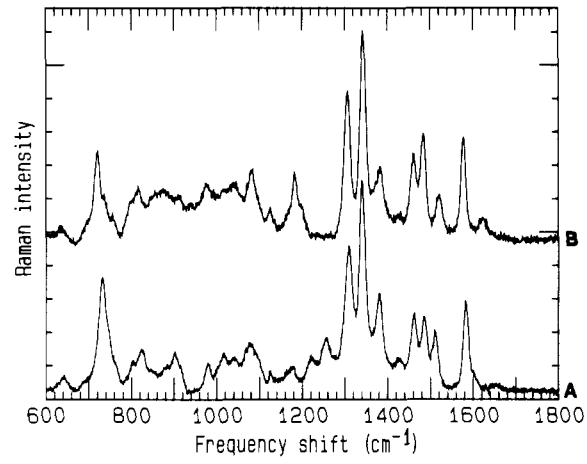

FIGURE 4: Effect of D_2O on the Raman spectrum of pA2′pA2′pA (A) in water, pH 6.6, and (B) in D_2O, pD 5.8. pH was estimated by spotting a small sample on pH paper.

Only the hydrogens attached to the exocyclic nitrogens of adenine and the ribose hydroxyls would be expected to be exchanged here at the pD of 6.6. Exchange of C8 and C2 protons of adenosine is much slower (Thomas et al., 1975, and references cited therein) and therefore probably did not occur in this experiment. A minor band at 1650 cm^{-1} in H_2O was shifted down in frequency to 1625 cm^{-1} in D_2O. This band may be related to the high-frequency mode found in substituted benzenes since adenine is an aromatic C6-substituted compound (Tsuboi et al., 1973). The band at 1254 cm^{-1}, assigned

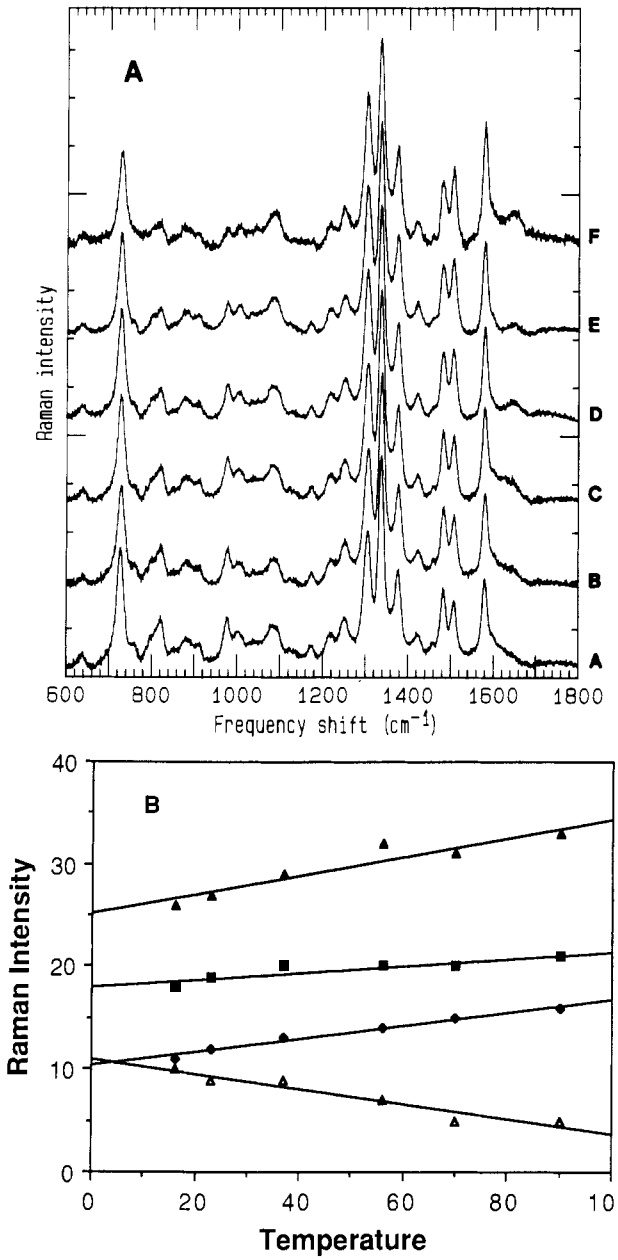

FIGURE 5: Effect of temperature on the Raman spectrum of pA2′pA2′pA. (A) Raman spectrum of pA2′pA2′pA, pH 7.3, was taken at (A) 16, (B) 23, (C) 37, (D) 56, (E) 70, and (F) 90 °C. (B) Raman intensities of the bands at (△) 823, (▲) 1308, (■) 1378, and (◆) 1510 cm^{-1}.

to the exocyclic N6 amino group of the adenine bases by Tsuboi et al. (1973), is not present in D_2O, indicating that this assignment is also correct for the 2′,5′-oligoadenylates. This further suggests that the N6 amino groups of adenine moieties of 2–5A do not participate in stable intermolecular interactions in solution.

Deuteriation resulted in the appearance of two new bands at 1182 and 1200 cm^{-1}. The 1182-cm^{-1} mode has been assigned to the ND_2 scissor by Tsuboi et al. (1973). The 1200-cm^{-1} band probably arises from adenine, since it also appears when AMP is deuteriated (Yue et al., 1986). Most bands above 1300 cm^{-1} also shifted down slightly in frequency as a result of changes in vibrational coupling. Numerous changes in the 700–900-cm^{-1} region of the spectrum, containing ribose and phosphate bands, were also observed.

Assessing Secondary Structure. Raman hyperchromism is observed in the spectra of ordered structures such as poly(rA) when the bases unstack at high temperature. Bands in

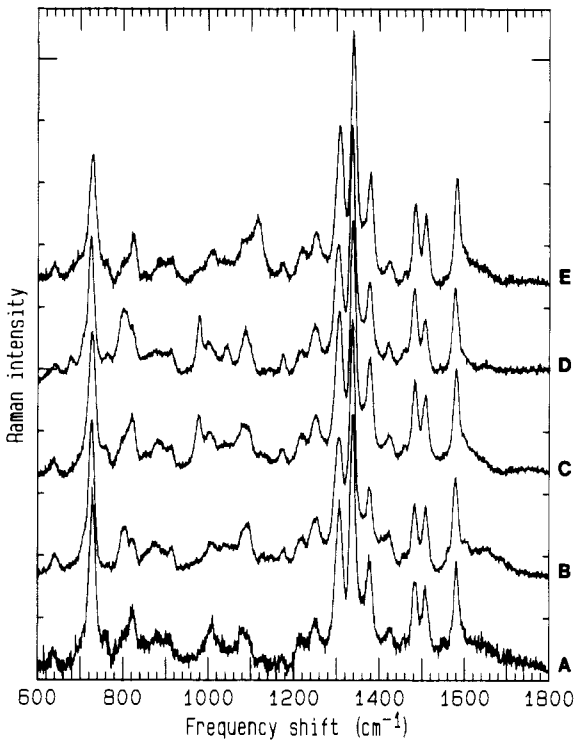

FIGURE 6: Comparison of the Raman spectra 2′,5′- and 3′,5′-oligoadenylates. Raman spectra were obtained in water, pH 7.3, as described under Materials and Methods. (A) A2′pA2′pA; (B) A3′pA3′pA; (C) pA2′pA2′pA, commercial source; (D) pA3′pA3′pA; (E) pppA2′pA2′pA.

Raman spectra of poly(rA) and A3′pA3′pA at 729, 1308, and 1510 cm^{-1} increase upon melting at 90 °C (Prescott et al., 1974).

Our studies at 16 °C and at higher temperatures enable us to make four observations (spectra discussed below were normalized to either the 1095-cm^{-1} O–P–O symmetric stretch or the 1338-cm^{-1} adenine bond). (1) We observed a linear increase in intensities of lines in the spectrum of pA2′pA2′pA at 1308, 1378, and 1510 cm^{-1} (21, 16, and 33%, respectively) with increasing temperature (Figure 5A). (2) The intensities of bands in the spectra of AMP and pA2′pA2′pA at 1308, 1378, and 1510 cm^{-1} at 16 °C were essentially the same (Figure 2). (3) The intensities of bands in the spectra of pA3′pA3′pA at 1308, 1378, and 1510 cm^{-1} were slightly decreased with respect to the same bands in AMP, which is consistent with observations by Prescott et al. (1974) (data not shown). (4) The 814-cm^{-1} line in the Raman spectrum of A3′pA3′pA at 20 °C shifts to 798 cm^{-1} at 90 °C and has been used as a measure of "disorder" (lack of secondary structure) in this and other 3′,5′-linked RNAs (Prescott et al., 1974). No shift of the 823-cm^{-1} line in the spectrum of pA2′pA2′pA was observed at 90 °C (Figure 5A).

Linkage Isomers. Spectra of A2′pA2′pA, A3′pA3′pA, and pA3′pA3′pA were examined to investigate the effect of the 2′,5′-phosphodiester bond on Raman active modes. The PO_3^{2-} mode at 980 cm^{-1} (Rimai et al., 1969) was observed for both pA2′pA2′pA and pA3′pA3′pA (Figure 6C,D). pA3′pA3′pA had well-resolved bands at 680 and 760 cm^{-1} (Figure 6D); these modes appeared as shoulders on the 729-cm^{-1} band of pA2′pA2′pA (Figure 6C). The ratio of the intensities at 1510 and 1482 cm^{-1} was smaller in 3–5A than in 2–5A (Figure 6). The major difference between A2′pA2′pA and A3′pA3′pA was in the frequency of the phosphodiester backbone bands found in the 800–825-cm^{-1} region of the spectrum (Figure 6). The Raman spectrum of 3′,5′-linked trimer core, A3′pA3′pA, re-

vealed the presence of a strong backbone mode at 802 cm^{-1} and a relatively weaker mode at 820 cm^{-1}. 2′,5′-Oligoadenylates contained both of these bands, but the band at 823 cm^{-1} was stronger and sharper relative to the 820-cm^{-1} band of 3–5A. The 2′,5′-oligoadenylate capable of activating the cellular endonuclease, pppA2′pA2′pA, had the sharpest band at 823 cm^{-1} (Figure 6E). The possible significance of these results is discussed below.

Discussion

Previously published physiochemical studies on the conformation of 2′,5′-linked oligoadenylates in solution have yielded mixed results. Studies using CD to estimate base stacking revealed that the hypochromicity of 2′,5′-oligoadenylates was higher than that of the corresponding 3′,5′-oligoadenylates (Sawai, 1983; Doornbos et al., 1981, 1983). This result suggests that 2′,5′-oligoadenylates possess more base stacking than 3′,5′-oligoadenylates. In contrast, a CD comparison of 2–5A and 3–5A tetramer, pentamer, and hexamer at 20 °C showed that $\Delta\epsilon$ for 3′,5′-oligoadenylates increases with increasing chain length but $\Delta\epsilon$ for 2′,5′-oligoadenylates remains constant with increasing chain length. The conclusion was that stacking in 2′,5′-oligoadenylates is weaker than in 3′,5′-oligoadenylates (Hirao et al., 1983; Dhingra & Sarma, 1978). X-ray analysis of the structure of crystals of A2′pC implied that a very compact right-handed helix can exist; intramolecular O4′ ribose–adenine stacking (rather than intermolecular base stacking) was proposed (Parthasarathy et al., 1982).

Our spectra were normalized to both the 1095-cm^{-1} PO_2^- band and the 1338-cm^{-1} adenine band. We observed no change in the relative intensities of these bands with temperature, indicating that the 1338-cm^{-1} band may be a good band to normalize to under these circumstances.

Spectra of pA2′pA2′pA and AMP have the same relative intensities (at 16 °C) in bands that are sensitive to base stacking (Figure 2), in contrast to observations made by Prescott et al. (1974) in a comparison of AMP and 3–5A core. This suggests that there is little or no base stacking in 2–5A. The relative intensities of bands at 1308, 1378, and 1510 cm^{-1} increased and the relative intensity of the 823-cm^{-1} band decreased as temperature was increased from 16 to 90 °C (Figure 5A). The linearity of these changes (Figure 5B) suggests that the 2–5A molecule was undergoing a change in structural equilibrium that is not related to base stacking. If base stacking was disrupted, changes in these bands would be expected to follow a typical melting curve, as observed for poly(A)·poly(U) (Small & Peticolas, 1971) and for GpC (Prescott et al., 1974).

pA3′pA3′pA but not A3′pA3′pA has weak but well-resolved bands at 680 and 760 cm^{-1} that were significantly less discernible in both A2′pA2′pA and pA2′pA2′pA (Figure 6). These bands are also not present in poly(rA) (Prescott et al., 1974). Rimai et al. (1969) assigned bands at these positions to the polyphosphate chain at the 5′-terminus of ADP and ATP because they were absent in AMP (see Figure 2). This assignment does not explain our results since pA3′pA3′pA does not contain polyphosphate. Preliminary studies of pA3′pA2′pA and pA2′pA3′pA have provided further clues to the nature of the 680- and 760-cm^{-1} bands in oligonucleotides. When the first ribose was 3′,5′-linked, as in pA3′pA2′pA, both the 680-and 760-cm^{-1} bands were present (not shown), as observed with pA3′pA3′pA (Figure 6D). However, when the first linkage was 2′,5′-linked, as in pA2′pA3′pA, the Raman spectrum appears similar to that of pA2′pA2′pA, which lacks well-resolved bands at 680 and 760 cm^{-1} (Figure 6C and

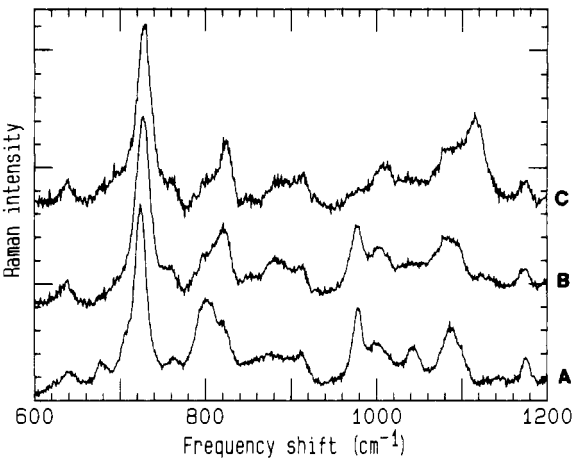

FIGURE 7: Comparison of the Raman phosphodiester backbone modes. (A) pA3′pA3′pA; (B) pA2′pA2′pA; (C) pppA2′pA2′pA.

results not shown). These results imply that the 680- and 760-cm^{-1} bands may arise from the presence of a phosphate at the 5′-terminus of certain oligonucleotides. Changes in backbone parameters such as the glycosyl torsion angle, which may accompany differences in the phosphodiester linkage, may account for the observed difference between 2′,5′- and 3′,5′-linked oligoadenylates.

Raman spectroscopy has been used to identify the ribose pucker of nucleic acids. A-genus DNA possesses a C3′-endo ribose conformation and has a strong sharp band in the 807–815-cm^{-1} region (Erfurth et al., 1972, 1975; Thomas & Hartman, 1973; Goodwin & Brahms, 1978). Raman spectra of B- and C-genus DNA have weak, broad bands at 835 and 875 cm^{-1}, respectively (Brown & Peticolas, 1975; Lu et al., 1975). For ribonucleotides, the Raman A-genus marker bands are shifted up about 7 cm^{-1} to 814–822 cm^{-1} (Erfurth et al., 1972, 1975; Goodwin et al., 1978; Hartman et al., 1973; Peticolas & Tsuboi, 1979). Marker modes have been shown to exist in low-temperature Raman scans of mononucleotides (Small & Peticolas, 1971) and in U3′pA, G3′pC, and dT3′pdT (Thomas & Peticolas, 1983). On the basis of these results Peticolas et al. (1983) proposed that the position of the phosphodiester backbone marker mode for ribonucleotides in the 814–822-cm^{-1} range depends on the coupling through the 5′-ribose ester linkage. Assignment of the 823-cm^{-1} line in the spectrum of 2–5A as resulting from phosphodiester group vibrations seems reasonable (Figure 6). Wartell and Harrell (1986) recently reported that an "extra" 823-cm^{-1} backbone band was required to reproduce the 800–850-cm^{-1} region of poly[d(A-T)]·poly[d(A-T)] by curve-fitting procedures. The relationship of this band to the clearly visible 823-cm^{-1} band in the Raman spectra of 2–5As has not been ascertained.

NMR studies have indicated that the ribose pucker of A2′pA2′pA is mixed at 20 °C, while the deoxy analogue, d(A2′pA2′pA), is almost exclusively C3′-endo at 20 °C (Doornbos et al., 1981, 1983). If a mixed population of ribose puckers is observed by NMR, on a time scale of 10^{-6} s, then Raman spectroscopy, on a time scale of $\leq 10^{-13}$ s, should identify these populations of ribose pucker.

We assign the band at 823 cm^{-1} to phosphodiester group vibrations in 2–5As (Figure 6). NMR evidence indicates that a mixture of ribose puckers exists in 2–5A. We observed a major band at 823 cm^{-1} and a minor band at 802 cm^{-1}. These bands may represent the relative predominance of one ribose pucker type over the other since the position of the backbone marker has been shown to be sensitive to furanose pucker (Thomas & Peticolas, 1983). The broadness or sharpness of

the band may also be influenced by furanose pucker. We proposed that the biologically active molecule, pppA2′pA2′pA, has a more uniform ribose pucker than pA2′pA2′pA, since the band at 823 cm^{-1} in pppA2′pA2′pA is substantially sharper than the 823-cm^{-1} band in pA2′pA2′pA (Figure 7). Alternatively, changes in other backbone torsion angles may affect the appearance of this band. In either case, the Raman spectra demonstrates that the backbone structure in the biologically active pppA2′pA2′pA differs from that found in nonbiologically active forms of 2–5A and 3′,5′-oligoadenylates.

2′,5′-Oligoadenylates probably present unique conformational properties that are important in binding and activating RNase L. Previous studies employing structural analogues of 2–5A have implicated the first 2′,5′-linkage as being critical for binding to RNase L. The observation that a brominated monophosphate analogue of 2–5A retained biological activity suggests that the 5′-triphosphate may not be an absolute requirement for RNase L activation. We are presently exploring the possibility that bromination forces the ribose of pA2′pA2′pA into a more rigid conformation as reflected by a sharp 823-cm^{-1} band. The rigidity of the phosphodiester backbone and possibly of the furanose pucker may be related to the ability of the 2′,5′-oligoadenylates to activate RNase L. These assignments reported here will also be useful in studying the interaction of 2′,5′-oligoadenylates with proteins.

Acknowledgments

We thank Dr. Paul F. Torrence for generously supplying many of the oligonucleotides used in this work and Sheila Loughran for assistance with the graphics programs.

Registry No. A2′pA2′pA, 70062-83-8; pA2′pA2′pA, 61172-40-5; pppA2′pA2′pA, 65954-93-0; AMP, 61-19-8; ATP, 56-65-5; A3′pA3′pA, 917-44-2; pA3′pA3′pA. 1684-34-0; adenosine, 58-61-7.

References

Baret, J. F., Carbone, G. P., & Sturm, J. (1979) *J. Raman Spectrosc. 8*, 291–304.

Benevides, J. M., & Thomas, G. J., Jr. (1983) *Nucleic Acids Res. 11*, 5747–5761.

Benevides, J. M., LeMeur, D., & Thomas, G. J., Jr. (1984) *Biopolymers 23*, 1011–1024.

Brown, E. B., & Peticolas, W. L. (1975) *Biopolymers 14*, 1259–1271.

Dhingra, M. M., & Sarma, R. H. (1978) *Nature (London) 272*, 798–801.

Doornbos, J., DenHartog, J. A., VanBoom, J. H., & Altona, C. (1981) *Eur. J. Biochem. 116*, 403–412.

Doornbos, J., Charubala, R., Pfleiderer, W., & Altona, C. (1983) *Nucleic Acids Res. 11*, 4569–4582.

Erfurth, S. C., Kiser, E. J., & Peticolas, W. L. (1972) *Proc. Natl. Acad. Sci. U.S.A. 69*, 938–941.

Erfurth, S. C., Bond, J., & Peticolas, W. L. (1975) *Biopolymers 14*, 1245–1257.

Fodor, P. A., Rava, R. P., Hays, T. R., & Spiro, T. G. (1985) *J. Am. Chem. Soc. 107*, 1520–1529.

Goodwin, D. C., & Brahms, J. (1978) *Nucleic Acids Res. 5*, 835–850.

Hartman, K. A., Lord, R. C., & Thomas, G. J., Jr. (1973) in *Physicochemical Properties of Nucleic Acids* (Duchesne, J., Ed.) Vol. 2, pp 92–143, Academic, New York.

Haugh, M. C., Cayley, P. J., Serfinoska, H., Norman, D. C., Reese, C. B., & Kerr, I. M. (1983) *Eur. J. Biochem. 132*, 77–84.

Hirao, I., Ishido, Y., & Miura, K. (1983) *Nucleic Acids Symp. Ser. 12*, 193–196.

Imai, J., & Torrence, P. F. (1985) *J. Org. Chem. 50*, 1418–1426.

Imai, J., Lesiak, K., & Torrence, P. F. (1985) *J. Biol. Chem. 260*, 1390–1393.

Johnston, M. I., & Torrence, P. F. (1984) in *Interferon* (Freidman, R. M., Ed.) Vol. 3, pp 189–298, Elsevier, New York.

Johnston, M. I., Hearl, W. G., White, J. C., Imai, J., Torrence, P. F., & Williams, R. W. (1985) *Prog. Clin. Biol. Res. 202*, 37–45.

Kerr, I. M., & Brown, R. E. (1978) *Proc. Natl. Acad. Sci. U.S.A. 75*, 256–260.

Kerr, I. M., Brown, R. E., & Ball, L. A. (1974) *Nature (London) 250*, 57–59.

Kimchi, A., Shure, H., Lapidot, Y., Rapoport, S., Panet, A., & Revel, M. (1981a) *FEBS Lett. 134*, 212–216.

Kimchi, A., Shure, A., & Revel, M. (1981b) *Eur. J. Biochem. 114*, 5–10.

Lebleu, B., Sen, G. C., Shaila, S., Carber, B., & Lengyel, P. (1976) *Proc. Natl. Acad. Sci. U.S.A. 73*, 3107–3111.

Lesiak, K., Imai, J., Floyd-Smith, G., & Torrence, P. F. (1983) *J. Biol. Chem. 258*, 13082–13088.

Lord, R. C., & Thomas, G. J., Jr. (1967) *Spectrochim. Acta, Part A 23A*, 969.

Lu, K. C., Prohofsky, E. W., & Van Zant, L. L. (1975) *Biopolymers 16*, 2491–2506.

Manfait, M., Theophanides, T., Alix, A. J. P., & Jeannesson, P. (1984) in *Spectroscopy of Biological Molecules* (Sandorfy, C., & Theophanides, T., Eds.) pp 113–136, Reidel, Dordrecht, Holland.

Parthasarathy, R., Malik, M., & Fridey, S. M. (1982) *Proc. Natl. Acad. Sci. U.S.A. 79*, 7292–7296.

Peticolas, W. L., & Tsuboi, N. (1979) in *Infrared and Raman Spectroscopy of Biological Molecules* (Theophanidies, T. M., Ed.) pp 153–165, Reidel, Dordrecht, Holland.

Prescott, B., Gamache, R., Liveramento, J., & Thomas, G. J., Jr. (1974) *Biopolymers 13*, 1821–1845.

Rimai, L., Cole, T., Parsons, J. L., Hickmott, J. T., Jr., & Carew, E. B. (1969) *Biophys. J. 9*, 320–329.

Savitsky, A., & Golay, M. (1967) *Anal. Chem. 36*, 1627–1639.

Sawai, H. (1983) *Nucleic Acids Symp. Ser. 12*, 189–192.

Sawai, H., Imai, J., Lesiak, K., Johnston, M. I., & Torrence, P. F. (1983) *J. Biol. Chem. 258*, 1671–1677.

Sen, G. C., LeBleu, B., Brown, G. E., Kawakita, M., Slattery, E., & Lengyel, P. (1976) *Nature (London) 264*, 370–373.

Shimanouchi, E. B., Tsuboi, M., & Kyogoku, Y. (1964) in *Chemical Physics* (Duchesne, J., Ed.) Vol. VII, pp 435–498, Interscience, London.

Small, E. W., & Peticolas, W. L. (1971) *Biopolymers 10*, 1377–1425.

Thomas, G. A., & Peticolas, W. L. (1983) *J. Am. Chem. Soc. 105*, 986–992.

Thomas, G. J., Jr., & Hartman, K. A. (1973) *Biochim. Biophys. Acta 312*, 311–322.

Thomas, G. J., Jr., & Livramento, J. (1975) *Biochemistry 14*, 5210–5218.

Torrence, P. F., & Lesiak, K. (1986) *J. Med. Chem. 29*, 1015–1022.

Torrence, P. F., Imai, J., & Johnston, M. I. (1981) *Proc. Natl. Acad. Sci. U.S.A. 78*, 5993–5997.

Torrence, P. F., Imai, J., Lesiak, K., Jamoulle, J. C., & Sawai, H. (1984) *J. Med. Chem. 27*, 726–733.

Torrence, P. F., Imai, J., Wong, A., & Lesiak, K. (1985) *Prog. Clin. Biol. Res. 202*, 75–80.
Tsuboi, M., Takahushi, S., & Harada, I. (1973) in *Physiochemical Properties of Nucleic Acids* (Duchesne J., Ed.) Vol. 2, p 91, Academic, New York.
Wartell, R. M., & Harell, J. T. (1986) *Biochemistry 25*, 2664–2671.
Williams, R. W. (1983) *J. Mol. Biol. 166*, 581–603.
Yue, T. K., Martin, C. L., Chen, D., Nelson, P., Sloan, D. L., & Chandler, R. (1986) *Biochemistry 25*, 4981–4987.

Photoaffinity Labeling of the Thymidine Triphosphate Binding Domain in *Escherichia coli* DNA Polymerase I: Identification of Histidine-881 as the Site of Cross-Linking†

V. N. Pandey,‡ K. R. Williams,§ K. L. Stone,§ and M. J. Modak*,‡

Department of Biochemistry, University of Medicine and Dentistry of New Jersey, New Jersey Medical School, Newark, New Jersey 07103, and Department of Molecular Biophysics and Biochemistry, Yale University School of Medicine, New Haven, Connecticut 06501

Received May 18, 1987; Revised Manuscript Received July 14, 1987

ABSTRACT: Using the technique of ultraviolet-mediated cross-linking of substrate deoxynucleoside triphosphates (dNTPs) to their acceptor site [Abraham, K. I., & Modak, M. J. (1984) *Biochemistry 23*, 1176–1182], we have labeled the Klenow fragment of *Escherichia coli* DNA polymerase I (Pol I) with [α-^{32}P]dTTP. Covalent cross-linking of [α-^{32}P]dTTP to the Klenow fragment is shown to be at the substrate binding site by the following criteria: (a) the cross-linking reaction requires dTTP in its metal chelate form; (b) dTTP is readily competed out by other dNTPs as well as by substrate binding site directed reagents; (c) labeling with dTTP occurs at a single site as judged by peptide mapping. Under optimal conditions, a modification of approximately 20% of the enzyme was achieved. Following tryptic digestion of the [α-^{32}P]dTTP-labeled Klenow fragment, reverse-phase high-performance liquid chromatography demonstrated that 80% of the radioactivity was contained within a single peptide. The amino acid composition and sequence of this peptide identified it as the peptide spanning amino acid residues 876–890 in the primary sequence of *E. coli* Pol I. Chymotrypsin and *Staphylococcus aureus* V8 protease digestion of the labeled tryptic peptide in each case yielded a single smaller fragment that was radioactive. Amino acid analysis and sequencing of these smaller peptides further narrowed the dTTP cross-linking site to within the region spanning residues 876–883. We concluded that histidine-881 is the primary attachment site for dTTP in *E. coli* DNA Pol I, since during amino acid sequencing analysis of all three radioactive peptides loss of the histidine residue at the expected cycle is observed.

The discovery, purification, and extensive characterization of *Escherichia coli* DNA polymerase I (*E. coli* Pol I)[1] by Kornberg and colleagues (Kornberg, 1969, 1982) led to the early groundwork which adequately describes the general nature of a typical DNA polymerase reaction in all life forms which contain DNA. The second important advance relates to the successful cloning of the gene for *E. coli* Pol I (Kelley et al., 1977; Murray & Kelly, 1979; Kelley & Stump, 1979) and its enzymatically active fragment (Klenow fragment) (Joyce & Grindley, 1982) which permitted the elucidation of the nucleotide sequence followed by the prediction and actual demonstration of the primary amino acid sequence (Joyce et al., 1982; Brown et al., 1982). The Pol I overproducer strain of *E. coli* essentially eliminated severe constraint on the availability of enzyme protein. The abundance of enzyme protein in turn culminated in the third important advance, namely, the elucidation of the crystal structure of this enzyme (Ollis et al., 1985). The solving of the Pol I crystal structure has opened a molecular window through which molecular aspects of polymerase and associated reactions catalyzed by this enzyme can be visualized.

The site-specific chemical modification of the enzyme followed by the identification of that site together with its functional attributes has been one of our approaches to relate the structure and function of DNA polymerase I. Thus, we have determined that a pyridoxal phosphate sensitive lysine (residue 758) is essential for substrate binding (Basu & Modak, 1987). Similarly, methionine-512 (Basu et al., 1987) and arginine-841 (Mohan et al., 1987) have been found to be important residues required in the template-primer binding function of this enzyme. Simultaneously, we also developed protocols for the affinity labeling of DNA polymerases, first using azido analogues of nucleotides (Abraham et al., 1983) and subsequently using the unsubstituted substrate dNTPs themselves as affinity labeling reagents (Modak & Giller-

† Supported by grants from the USPHS–National Institute of General Medical Sciences (NIH-NIGMS-36307 and NIH GM 31539).
* Address correspondence to this author.
‡ New Jersey Medical School.
§ Yale University School of Medicine.

[1] Abbreviations: Pol I, *Escherichia coli* DNA polymerase I; dNTP, deoxynucleoside triphosphate; EDTA, ethylenediaminetetraacetic acid; Tris-HCl, tris(hydroxymethyl)aminomethane hydrochloride; HPLC, high-performance liquid chromatography; TPCK, tosylphenylalanine chloromethyl ketone; PTH, phenylthiohydantoin; DMPTU, *N,N*-dimethyl-*N*-phenylthiourea; DPTH, *N,N'*-diphenylthiourea; SDS, sodium dodecyl sulfate.

0006-2960/87/0426-7744$01.50/0